

VĚDECKÉ SPISY VYSOKÉHO UČENÍ TECHNICKÉHO V BRNĚ

*Edice PhD Thesis, sv. 794*

*ISSN 1213-4198*

*thesis* IS

*Ing. David Štefan*

**Study of the Dissipation  
in Spiraling Vortical Structures**

VYSOKÉ UČENÍ TECHNICKÉ V BRNĚ  
FAKULTA STROJNÍHO INŽENÝRSTVÍ  
ENERGETICKÝ ÚSTAV  
ODBOR FLUIDNÍHO INŽENÝRSTVÍ VICTORA KAPLANA

**Ing. David Štefan**

**STUDY OF THE DISSIPATION  
IN SPIRALING VORTICAL STRUCTURES**

**STUDIUM DISIPACE SPIRÁLNÍCH VÍROVÝCH STRUKTUR**

Zkrácená verze Ph.D. Thesis

Obor: Konstrukční a procesní inženýrství  
Školitel: doc. Ing. Pavel Rudolf, Ph.D.  
Oponenti: doc. Ing. Sylva Drábková, Ph.D.  
Ing. Jiří Koutník, Dr.  
Ing. Aleš Skoták, Ph.D.  
Datum obhajoby: 3. listopadu 2015

**Keywords:**

dissipation, swirling flow, coherent structure, spiral vortex, vortex rope, vortex breakdown, diffuser, draft tube, cavitation, pressure pulsations, POD, OpenFOAM, LDA.

**Klíčová slova:**

disipace, vířivé proudění, koherentní struktura, spirální vír, vírový cop, rozpad víru, difuzor, sací trouba, kavitace, tlakové pulzace, POD, OpenFOAM, LDA.

**Místo uložení práce:**

VUT v Brně, Fakulta strojního inženýrství, Technická 2896/2,  
616 69 Brno, Česká Republika

© David Štefan, 2015

ISBN 978-80-214-5304-3

ISSN 1213-4198

# CONTENT

1 INTRODUCTION.....	5
2 MOTIVATION AND SCOPE OF THE PRESENT WORK.....	6
3 THEORY AND APPLIED METHODS .....	7
3.1 Laser Doppler anemometry (LDA) .....	8
3.2 Computational FluidS Dynamics (CFD) .....	8
3.3 Proper orthogonal decomposition.....	8
3.4 Energetic assessment .....	9
4 TEST CASES.....	9
4.1 Swirl generator apparatus designed at Brno university of technology (“BUT”) .....	9
4.2 Swirl generator apparatus designed at “Politehnica” University of Timisoara (“UPT”) ..	10
PART I - INVESTIGATION OF SWIRLING FLOW GENERATED BY THE “BUT” SWIRL GENERATOR .....	11
5 VELOCITY MEASUREMENTS IN THE CONICAL DIFFUSER.....	11
6 UNSTEADY PRESSURE PULSATIONS .....	11
7 HIGH SPEED CAMERA RECORDING OF THE CAVITATING VORTEX ...	12
8 CFD CALCULATION OF “BUT” SWIRL GENERATOR .....	13
9 COMPARISON OF EXPERIMENTAL MEASUREMENTS AND NUMERICAL RESULTS .....	14
9.1 Time evolution of numerically computed spiral vortex .....	14
9.2 Comparison of velocity results.....	15
10ENERGY DISSIPATION IN THE DOWNSTREAM PART OF THE DIFFUSER .....	16
PART II POD ANALYSIS.....	17
11POD ANALYSIS OF “BUT” SWIRL GENERATOR .....	17
11.1 POD of numerically computed pressure fields .....	18
12POD ANALYSIS OF “UPT” SWIRL GENERATOR WITH THE AXIAL WATER INJECTION .....	18
12.1 Numerical set-up .....	19
12.2 Decelerated swirling flows with the axial water injection.....	19
12.3 5% jet discharge .....	20
13CONCLUSIONS .....	22
LITERATURE .....	25
CURRICULUM VITAE .....	29
ABSTRACT.....	30



# 1 INTRODUCTION

The control of energy distribution and electricity production are in last several years considerably influenced by the electricity produced from the renewable sources highly depending on changes in weather conditions i.e. solar power plants and wind power plants. The pump storage hydro power plants (PSHPP) are proved to be effective for reduction of voltage and frequency fluctuations in whole power distribution grid. The control ability of PSHPP is connected with operation of a turbine in an extended area of flow rates  $Q$  quite far from the best efficiency point (BEP). Unfortunately, operation of the Francis turbine with a constant pitch of turbine runner (mainly used for the PSHPP) at partial discharge (off-design conditions where the flow rate  $Q < Q_{BEP}$ ) or overload (off-design conditions where the flow rate  $Q > Q_{BEP}$ ) is connected with occurrence of highly swirling flow at the inlet of the draft tube (outlet diffuser downstream of turbine runner) with a formation of so called vortex rope, see Figure 1. The vortex rope evolution correlates with a vortex breakdown and leads to the high pressure fluctuations in the draft tube [7], [44]. This draft tube surge propagates pressure pulsations into whole hydraulic system eventually leading to the runner blades breakdown [8] and may cause power swing phenomena at the electric generator [6]. Moreover, when the frequency of the pressure pulsations generated by the vortex rope rotation corresponds with a natural frequency of machine unit, it can enforce restrictions of turbine operation [7].

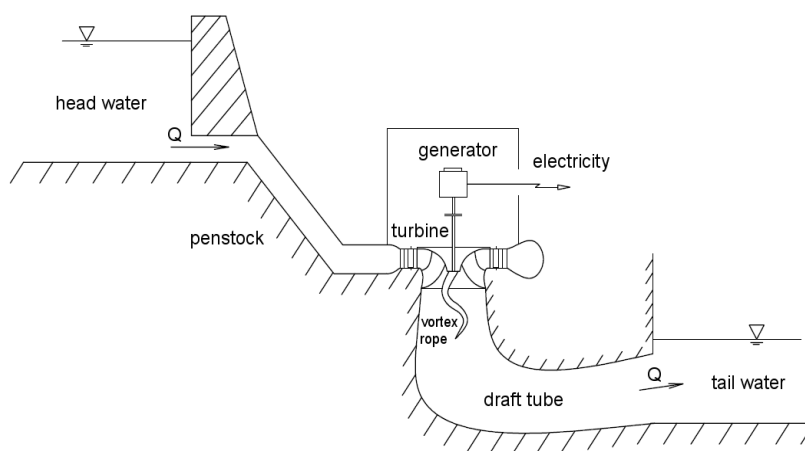


Figure 1 Schematic cross section of hydraulic power plant

In many cases of industrial fluid flows the flow instability called vortex breakdown occurs as a consequence of mechanisms in decelerated swirling flow. The vortex breakdown can be found in several forms related to the character of particular flow. Nevertheless, many forms of the vortex breakdown are not relevant to the industrial applications, e.g. bubble form of the vortex breakdown in low-Re flows. In case of hydraulic turbines with constant pitch of the runner, the high Reynolds number spiral form of the vortex breakdown appears, when the turbine is operated at part load  $Q < Q_{BEP}$ .

Despite the large database [16], covering investigations of the vortex breakdown during the last forty five years and extensive theoretical, experimental and computational research, we still lack deeper understanding of all influences on origin of this phenomena and their direct relations to the vortex rope properties (instability trigger, frequency of the precessing motion, helix shape, pressure amplitudes, etc.) [32].

Susan-Resiga et al. [39] concluded that the most significant case of the vortex breakdown in conical diffusers is a high Re spiral shape with central quasi stagnant region. They concluded, that the vortex breakdown in conical diffusers is a mechanism for limiting the increase in the swirl number

$$S_n = \frac{\int v_{ax} v_{tan} r dS}{R \int v_{ax}^2 dS} \quad (1.1)$$

and it occurs once the axial flux of circumferential moment of momentum is large enough with respect to the axial flux of axial momentum.

## 2 MOTIVATION AND SCOPE OF THE PRESENT WORK

Despite the large amount of research concerns with the decelerated flow in the draft tube of hydraulic turbines where the precessing vortex rope appears, many related phenomena are not fully clarified and described, e.g. main trigger causing flow instability leading to the vortex rope formation.

Besides the deeper understanding of the vortex rope phenomena developed during past decades, methodology to suppress this undesired flow features for turbomachinery is still sought and remains an object of interest. For these reasons a passive as well as an active (in form of external energy source) control methods for the vortex rope mitigation were introduced [42]. The passive control methods include fins mounted on the draft tube cone [21], [19], extension cones mounted on the runner crown [43], [28] or J-grooves [14], [15]. On the other hand, the active control methods include air injections either downstream (through the runner cone) or upstream (through the wicket gates trailing edge) of the runner [42], [26], tangential water jets at the discharge cone wall [13], axial water jet injection along the axis [41] and two-phase air-water jet injection along the axis [12].

Two ways of the draft tube flow investigations can be chosen. The first one utilizes full turbine model and can be used to provide clearly specified flow conditions of the draft tube flow for full range of operating points and a specific runner geometry. Nevertheless this approach is very demanding on financial sources and available facilities. Therefore the second way with the simplified swirl generator apparatus was employed. Basically the swirl generator is used to imitate flow conditions similar to ones in the draft tube cone of the Francis turbine.

The base of this thesis investigates flow behind two different swirl generator apparatus. While the first one (“BUT” swirl generator) was designed at our

department the second one (“UPT” swirl generator) is outcome of the research of the hydraulic group from the Politehnica University of Timisoara in Romania. The detailed description of both swirl generators is presented in section 4 . Consequently this thesis is later divided into two main parts, each of them devoted to study of the flow produced by the particular generator.

In the first part the comprehensive experimental and numerical investigation of swirling flow is carried out using the “BUT” swirl generator apparatus. Both the energy and dynamical aspects of the resulting swirling flow with the spiral vortical structure are accessed using the methods summarized in section 3 and aims to bring a new findings and summaries to the field of spiral vortex breakdown.

In the second part the POD technique shortly described in section 3.3 is applied to both “BUT” swirl generator and “UPT” swirl generator in order to assess the energy-dynamical description of these decelerated flows based on the spatio-temporal information extracted by the POD technique.

It is POD which allows better understanding of the flow behavior. For example strong advantage of POD applied on 2D or 3D flow fields in comparison with FFT obtained from the signal in the discrete points is that POD provides complete spatial representation of modes besides only temporal view obtained by FFT. This brings new view for research of decelerated swirling flows. In last several years the POD technique started to be widely used for full range of applications. The medical application of POD for transient turbulent flow over one cardiac cycle is presented in [9]. The civil engineering application of POD for turbulent flow inside a street canyon was investigated in [11]. The applications of POD analysis to extract the vortex shedding in the near wake of cylinder are presented in [25] and [27]. Several studies are concerned with turbulent jets [18] and swirling jets undergoing vortex breakdown [22], [23].

The utilization of POD in the field of turbomachinery is relatively new and was first introduced by our department [29], [30], [33]. One of the outcomes of this thesis is comprehensive utilization of POD for the study of the swirling flows where the spiral vortical structure appears. Moreover in case of the “UPT swirl generator” the results of POD analysis presented in section 12 are used to study possible ways to control and mitigate the vortex rope development in the draft tube of real hydraulic turbines and enhance overall turbine efficiency and operation reliability. The active control method in a form of axial water jet injection along the diffuser axis is utilized.

The POD analysis of “UPT” swirl generator is consequence of the collaborative work established during my internship at Politehnica University of Timisoara in 2012.

### **3 THEORY AND APPLIED METHODS**

Since the proposed study is based on both the experimental measurements and the numerical calculations the wide range of available methods are utilized.



### 3.1 LASER DOPPLER ANEMOMETRY (LDA)

The Laser Doppler Anemometer, or LDA, is a widely accepted tool for fluid dynamic investigations.

### 3.2 COMPUTATIONAL FLUIDS DYNAMICS (CFD)

Nowadays the computational fluid dynamic and relevant commercial software codes are well known and widely used for broad range of fluid flows applications. In this thesis both the commercial CFD software ANSYS Fluent and open source CFD code OpenFOAM are used.

While the numerical simulation of “BUT” swirl generator is carried out using OpenFOAM in version 2.2.2 the ANSYS Fluent R14 was used for calculation of “UPT” swirl generator.

For generation of computational grids of both “BUT” and “UPT” swirl generators the Gambit software was used.

Both calculations employ the Reynolds Average Navier-Stokes approach together with specified turbulence models. Two kinds of turbulence models are used. While for the calculation of “BUT” swirl generator using the OpenFOAM the realizable  $k-\varepsilon$  turbulence model is considered the calculation of “UPT” swirl generator is carried out with the Reynolds stress model (RSM) which is well implemented in ANSYS Fluent.

### 3.3 PROPER ORTHOGONAL DECOMPOSITION

Proper orthogonal decomposition (POD) was introduced into the field of fluid mechanics by Lumley [17], [2] as a technique which enables to bridge time and frequency domains and obtains spatio-temporal information about the flow in form of spatio-temporal eigenfunctions. POD provides a basis for the modal decomposition of a set of functions and most efficient way of capturing the dominant components, i.e. coherent structures. The POD can be used to analyze experimental as well as numerical data being applied to scalar or vectorial functions.

The scalar function  $p(\mathbf{x}, t_k)$ , e.g. pressure field, is considered in the following theoretical explanation. For instance, a set of data  $p(\mathbf{x}, t_k)$  as a function of physical space  $\mathbf{x}$  and discrete time  $t_k$ , can be expressed using POD as a set of orthogonal spatial basis functions  $\phi_i^k(\mathbf{x})$  (i.e. spatial modes), and temporal functions  $a_k(t_k)$  (i.e. temporal modes), respectively. Where  $i = 1, 2, \dots, N$ ,  $N$  is the number of grid points and  $k = 1, 2, \dots, M$ ,  $M$  is the number of snapshots. Accordingly, the approximation of the data set onto the first  $k$  snapshots can be written in terms of the spatial and temporal functions as follows

$$\hat{p}_i(\mathbf{x}, t_k) = \sum_{k=1}^K a_k(t_k) \phi_i^k(\mathbf{x}) \quad (3.1)$$

where  $K < M$  and approximation onto the first  $K$  functions has the largest mean square projection [9].

In method of snapshots suggested by Sirovich [36], the general  $N \times N$  eigenvalue problem is reduced to  $M \times M$  eigenvalue problem.

### 3.4 ENERGETIC ASSESSMENT

The main purposes to use the draft tube for the reaction turbine are that the turbine can be placed above the level of the tail water without losses of available head and transformation of residual kinetic energy at the turbine outlet into the static pressure thereby increasing overall turbine efficiency. In order to assess energetic performance of the diffuser the hydraulic efficiency  $\eta$ , pressure recovery coefficient  $c_p$  and hydraulic loss coefficient  $\xi$  will be evaluated.

$$\eta = \frac{p_{s(2)} - p_{s(1)}}{p_{d(1)} - p_{d(2)}} \quad (3.2)$$

$$c_p = \frac{p_{s(2)} - p_{s(1)}}{\frac{1}{2} \rho \alpha_{(1)} \bar{v}_{(1)}^2} \quad (3.3)$$

$$\xi = \frac{2}{\bar{v}_{(2)}^2} \left[ \left( \frac{\alpha_{(1)} \bar{v}_{(1)}^2 - \alpha_{(2)} \bar{v}_{(2)}^2}{2} \right) + \frac{p_{s(1)} - p_{s(2)}}{\rho} \right] \quad (3.4)$$

## 4 TEST CASES

The main part of present study is carried out for a test case of decelerated swirling flow in conical diffuser as a component of swirl generator apparatus included in a test rig situated in a hydraulic laboratory of V. Kaplan Department of Fluid Engineering. Additionally, due to collaborative reasons, the part of the study is concerned with a test case of swirl generator apparatus developed by research group at “Politehnica” University of Timisoara in Romania.

### 4.1 SWIRL GENERATOR APPARATUS DESIGNED AT BRNO UNIVERSITY OF TECHNOLOGY (“BUT”)

The swirl generator apparatus consists of two main parts, the swirl generator itself and the conical diffuser. The swirl generator was designed so that it converts fully axial flow into flow with significant tangential component. Ten stationary blades are situated on the inner spike which acts as a hub. The trailing edge deflection from axial direction is 30 degrees at spike side and linearly changes to 50 degrees towards outer wall. The blade length is 40 mm and blade thickness is 1 mm. The conical diffuser is connected downstream of the swirl generator. The inlet to the diffuser cone is 115 mm behind the blade trailing edge. The longitudinal cross-section through the swirl generator apparatus is shown in Figure 2.

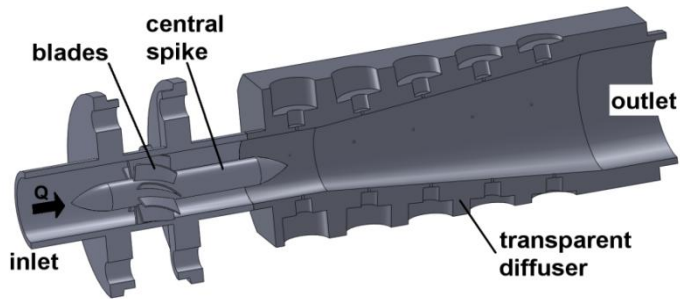


Figure 2 Scheme of swirl generator apparatus

#### 4.2 SWIRL GENERATOR APPARATUS DESIGNED AT “POLITEHNICA” UNIVERSITY OF TIMISOARA (“UPT”)

This swirl generator apparatus has been developed at “Politehnica” University of Timisoara (UPT) as a simplified device for experimental investigation of decelerated swirling flow with self-induced instability (e.g. precessing helical vortex). The swirl generator apparatus is installed in the test rig with a closed loop hydraulic circuit described in [3]. The swirl generator provides at cone inlet a flow similar to the one encountered in the draft tube of Francis turbine operated at partial discharge, e.g. at 70% of the best efficiency point [38]. The swirl apparatus test section is shown in Figure 3 with position of pressure transducers marked as MG0 – MG3. Detailed information about design and manufacturing of the swirl generator can be found in [40], [4]. The axial water injection through the turbine hub into the draft tube cone was introduced by Susan-Resiga et al. [41] as an active control technique for vortex rope mitigation in hydraulic turbines. This technique is well integrated in swirl generator apparatus for experimental investigation on simplified test case.

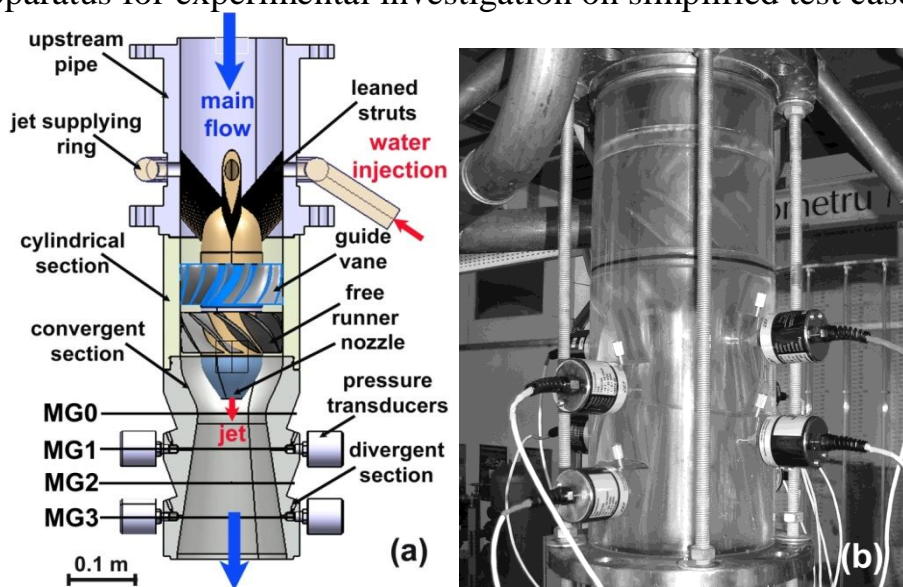


Figure 3 Swirl generator apparatus installed on the experimental test rig: a cross section (a) and a general view (b)

## PART I - INVESTIGATION OF SWIRLING FLOW GENERATED BY THE “BUT” SWIRL GENERATOR

### 5 VELOCITY MEASUREMENTS IN THE CONICAL DIFFUSER

The LDA (Laser Doppler Anemometry) measurements were performed in three cross-sections through the diffuser cone for the flow rates ensuring non-cavitation regimes. The axial and tangential velocities were measured simultaneously starting 2 mm from the diffuser cone wall and going perpendicularly to the diffuser axis with the 2 mm step for the axial velocity. The velocity measurements were carried out in three locations  $S1 = 23$  mm,  $S2 = 50$  mm and  $S3 = 75$  mm from the beginning of the diffuser cone, see Figure 4. The measured flow rates are  $Q = 5, 7, 8$  and  $11.5$  l/s. Note that velocities for flow rate  $Q = 11.5$  l/s were measured only in  $S2$  and  $S3$  cross-sections.

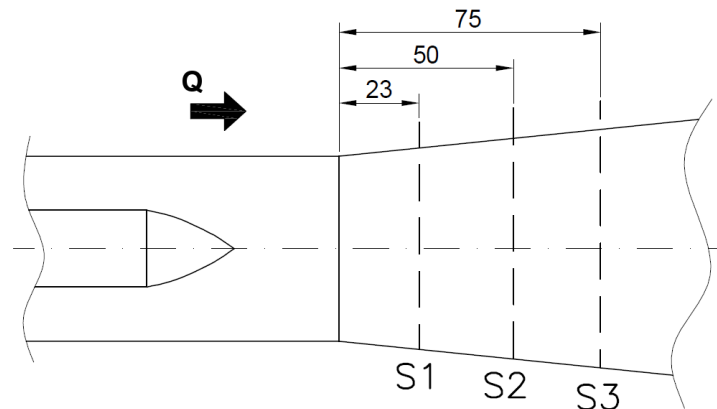


Figure 4 Locations of LDA measurements

### 6 UNSTEADY PRESSURE PULSATIONS

The unsteady pressure pulsations are measured in seven locations  $p0 - p6$ . The first pressure sensor  $p0$  is situated in front of the swirl generator apparatus in distance of 591 mm from the cone inlet, the five pressure sensors are situated in the conical diffuser (sensor  $p1$  is situated in front of the cone and  $p2 - p5$  are situated in

the cone) and  $p_6$  is placed downstream in the outlet of the diffuser in the distance of 291 mm downstream of cone inlet. The overall view of sensors locations can be seen in Figure 5.

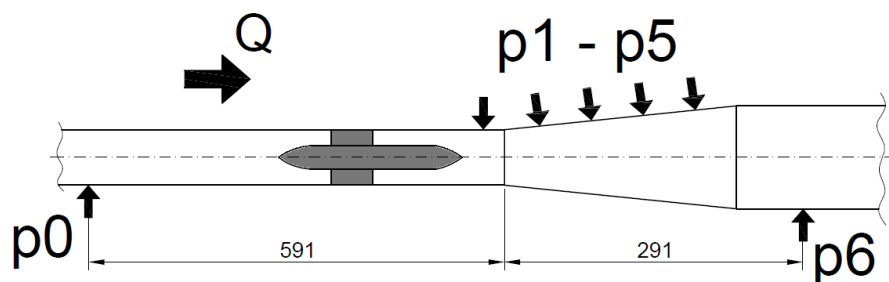


Figure 5 Sensors locations  $p_0$  and  $p_6$  situated in front of swirl generator and at the outlet of the diffuser

In order to evaluate asynchronous pulsations in all cross-sections for identical flow rate all five cross-sections are equipped by two oppositely oriented pressure sensors at the same time.

For this measurement the pressure sensors ( $p_1^*$  -  $p_5^*$ ) were included creating oppositely oriented row ( $180^\circ$  shifted in circumferential direction, see Figure 6). This enables to separate pulsations propagated either in longitudinal or in transverse direction in all five cross-sections for identical flow rate.

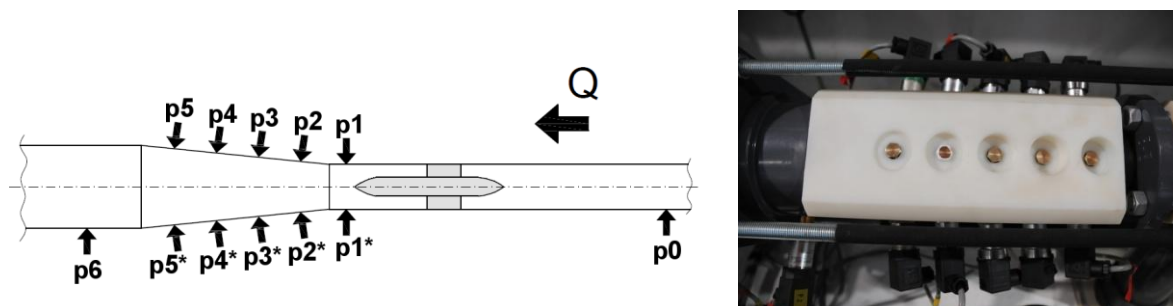


Figure 6 Measurements with fully equipped pressure sensors in two oppositely oriented rows

## 7 HIGH SPEED CAMERA RECORDING OF THE CAVITATING VORTEX

When the static pressure in the vortex core drops below the value of saturated vapor pressure the cavitation appears. Due to the light reflection the vortex core is well visible. In this case the cavitating vortex occurs at flow rates higher than  $Q = 7$  l/s. In order to experimentally investigate the behavior of the cavitating vortex structure the ensembles of the instantaneous images were recorded using the high speed camera.

The spiral vortex generated by the “BUT” swirl generator behaves unstably in time. The spiral rolls up and decays periodically generating the synchronous pressure pulsations propagated upstream. The unstable movement can be seen in Figure 7 where the time evolution of cavitating vortex at flow rate  $Q = 13.5$  l/s is

shown in selected time periods. At time  $t = 0$  sec the fully developed spiral vortex is observed. The rotating spiral vortex disintegrates ( $t = 0.013 - 0.021$  sec) leading to the short straight vortex ( $t = 0.034$  sec). Due to swirling flow instability the straight vortex later breaks up into spiral shape again ( $t = 0.058 - 0.108$  sec).

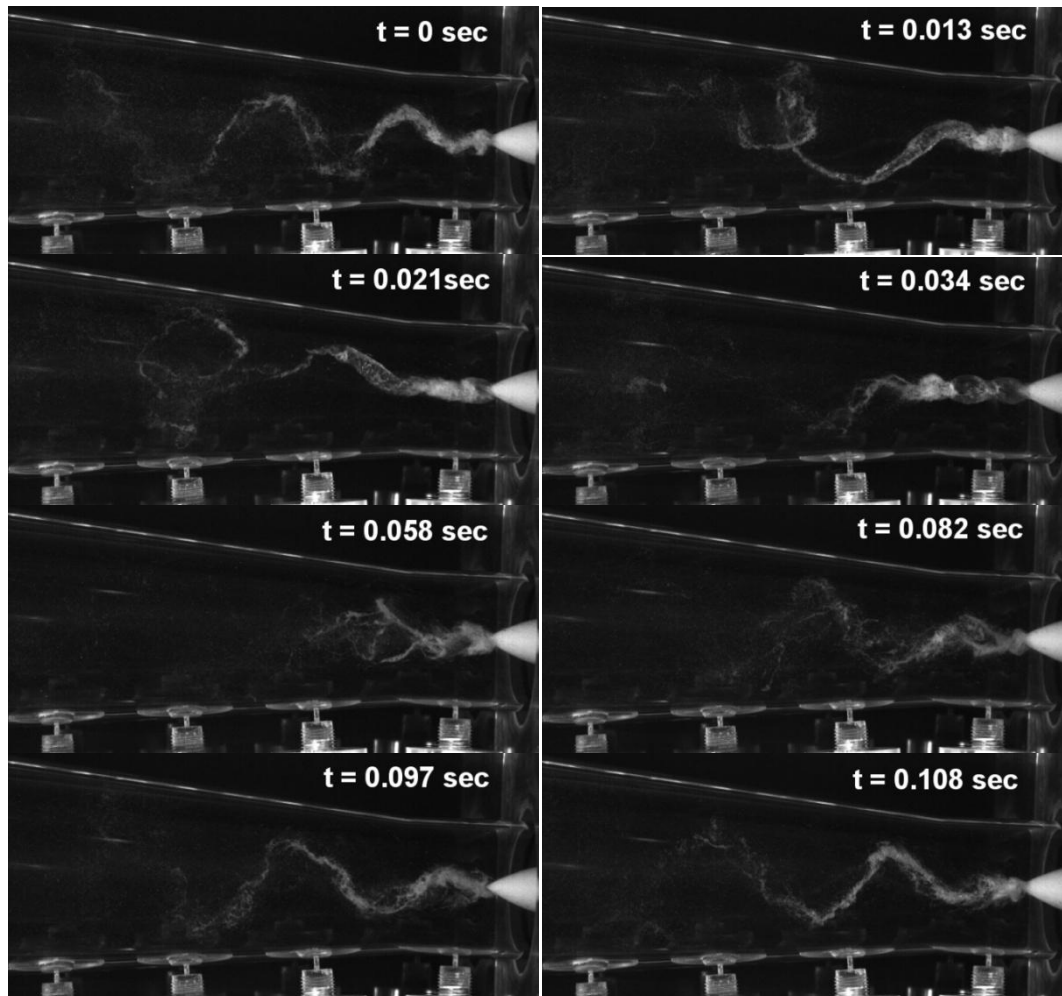


Figure 7 Time evolution of the vortex structure at flow rate  $Q = 13.5$  l/s

## 8 CFD CALCULATION OF “BUT” SWIRL GENERATOR

The numerical simulation of “BUT” swirl generator is carried out using OpenFOAM in version 2.2.2. The realizable  $k-\epsilon$  turbulence model (realizableKE) is used. The values of turbulent quantities - turbulent kinetic energy  $k$  and turbulent dissipation rate  $\epsilon$  were computed considering 5% of turbulent intensity at the inlet boundary. At the inlet boundary the fixed value of velocity according to the flow rate and at the outlet boundary the fixed value of pressure  $p = 0$  Pa are prescribed.

## 9 COMPARISON OF EXPERIMENTAL MEASUREMENTS AND NUMERICAL RESULTS

The comparison of pressure recovery factor is carried out for particular computed flow rates, see Figure 8.

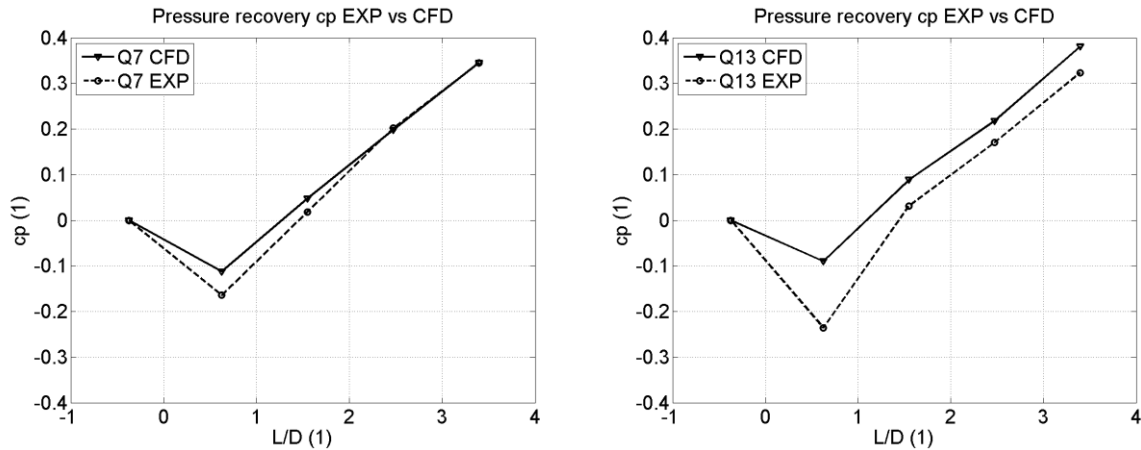


Figure 8 Pressure recovery factor EXP vs. CFD

The numerically computed frequencies of the vortex rotation are compared with ones extracted from the experimentally measured pressure signal, see Figure 9. The decomposition to the synchronous and asynchronous pressure pulsations is done for both experimental and numerical data.

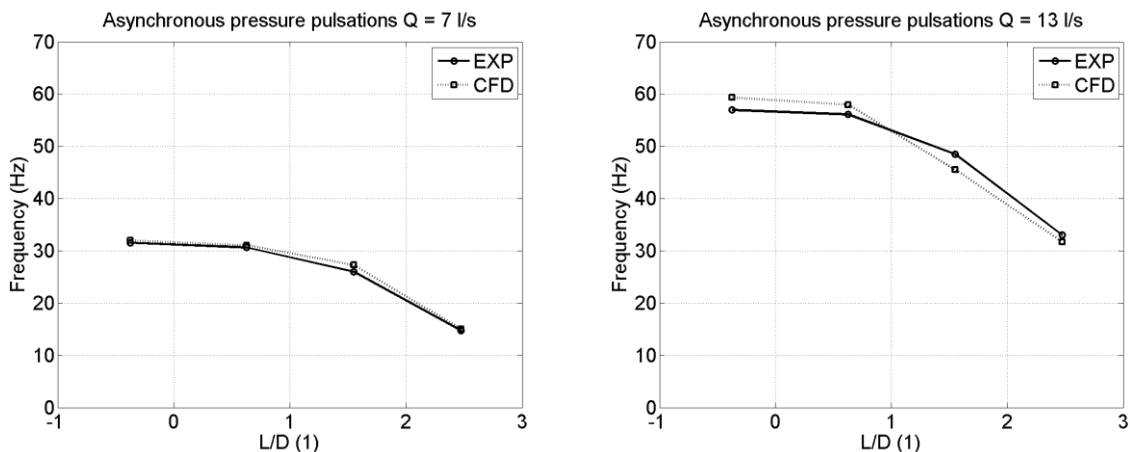


Figure 9 Asynchronous pressure pulsations at flow rate  $Q = 7$  l/s (left) and 13 l/s (right)

### 9.1 TIME EVOLUTION OF NUMERICALLY COMPUTED SPIRAL VORTEX

According to visual observations of cavitating vortex (see section 7 ) the time-evolution of numerically computed vortex structure (represented as the iso-contour of low static pressure) is carried out in Figure 10.

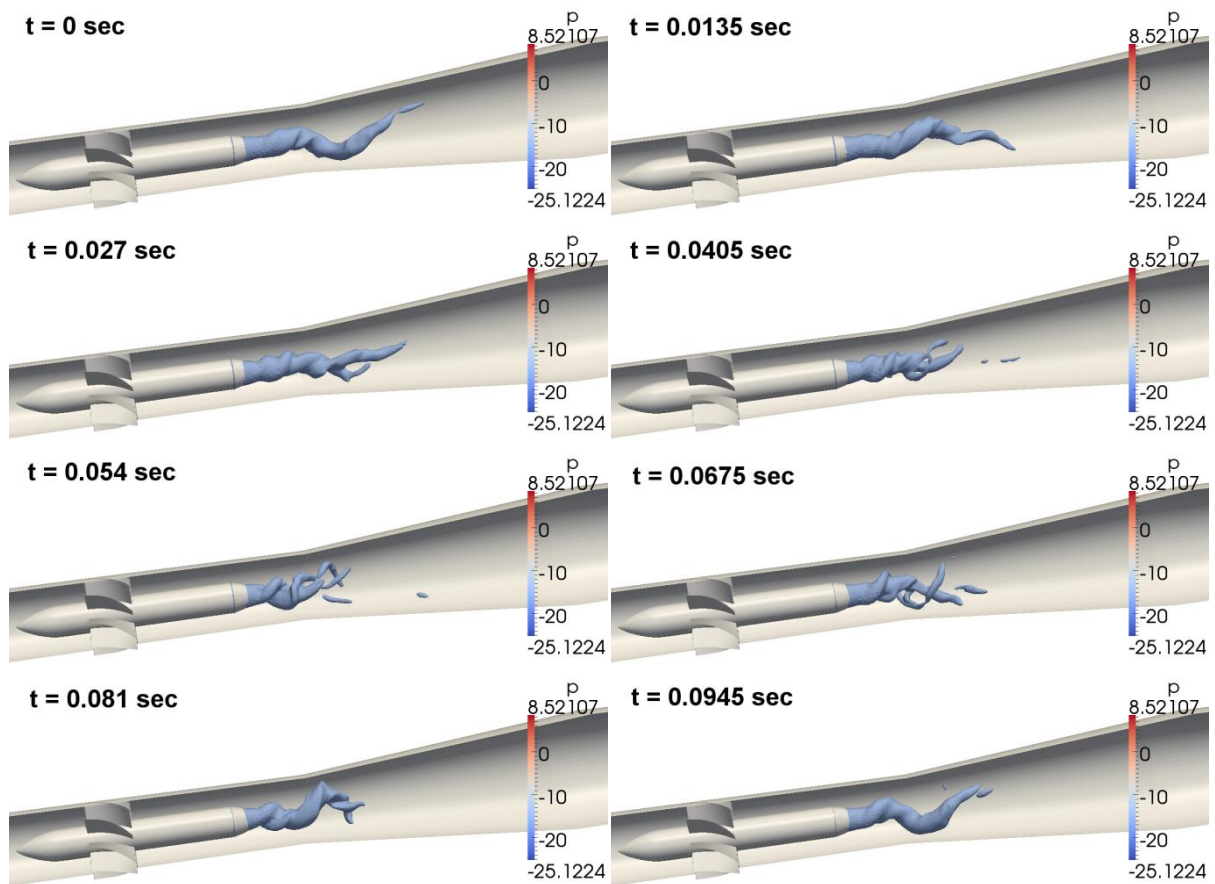


Figure 10 Time evolution of numerically computed vortex structure at flow rate  $Q = 7$  l/s (iso-contour of static pressure)

## 9.2 COMPARISON OF VELOCITY RESULTS

The comparisons of computed and measured axial and tangential velocity profiles in the first two cross-sections S1 and S2 are plotted in Figure 11 for  $Q = 7$  l/s.

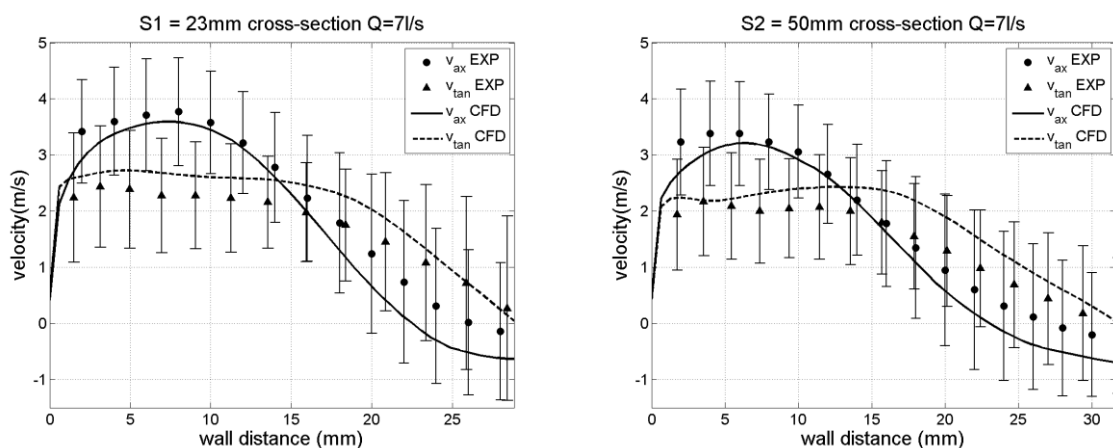


Figure 11 Comparison of measured and computed velocity profiles for flow rate  $Q = 7$  l/s



## 10 ENERGY DISSIPATION IN THE DOWNSTREAM PART OF THE DIFFUSER

On the base of irreversible part of stress tensor  $\Pi_{ij} = 2\mu v_{ij} + b\delta_{ij}v_{kk}$  arising from the Navier-Stokes equation the dissipation function  $\mathcal{D}$ , which represents power dissipated in the volume of fluid is calculated using equation

$$\mathcal{D} = \iiint_V \Pi_{ij} \frac{\partial v_i}{\partial x_j} dV \quad (10.1)$$

Using the tensor operations the equation (10.1) can be further expressed into final form of dissipation function  $\mathcal{D}$

$$\mathcal{D} = 2 \iiint_V \left\{ (\mu + \mu_t) \left[ \left( \frac{\partial v_x}{\partial x} \right)^2 + \frac{1}{2} \left( \frac{\partial v_x}{\partial y} + \frac{\partial v_y}{\partial x} \right)^2 + \frac{1}{2} \left( \frac{\partial v_x}{\partial z} + \frac{\partial v_z}{\partial x} \right)^2 + \left( \frac{\partial v_y}{\partial y} \right)^2 + \frac{1}{2} \left( \frac{\partial v_y}{\partial z} + \frac{\partial v_z}{\partial y} \right)^2 + \left( \frac{\partial v_z}{\partial z} \right)^2 \right] \right\} dV \quad (10.2)$$

The dissipation calculated in a form of dissipation function (10.2) should be in agreement with the power loss  $\Delta P$  between domain inlet and outlet calculated from the specific energy difference  $\Delta Y$ .

$$\Delta P = \rho \cdot Q \cdot \Delta Y = \rho \cdot Q \left( \frac{p_{inlet} - p_{outlet}}{\rho} + \frac{\alpha_{inlet} \cdot v_{inlet}^2 - \alpha_{outlet} \cdot v_{outlet}^2}{2} \right) \quad (10.3)$$

Comparison of resulting dissipation function  $\mathcal{D}$  with power loss  $\Delta P$  is plotted in Figure 12.

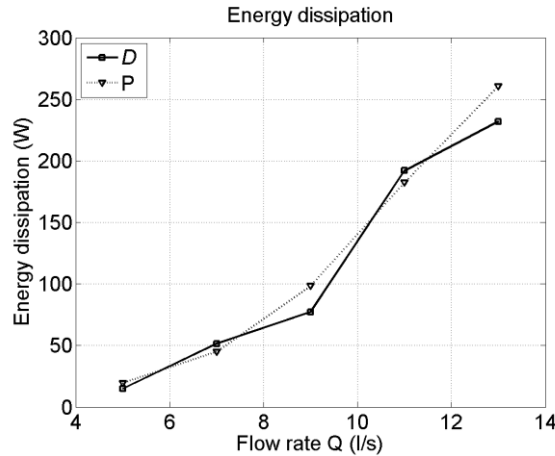


Figure 12 Power dissipated in the volume of fluid

## PART II POD ANALYSIS

### 11 POD ANALYSIS OF “BUT” SWIRL GENERATOR

The POD of cavitating vortex structure is carried out using the image ensembles recorded by the high speed camera. The grayscale images are post-processed in MATLAB<sup>®</sup>. In this case the cavitation (respectively the concentration of the vapor) is represented by the number (representing color scale) in interval from 0 (water) to 255 (vapor). In Figure 13 the spatial shapes of cavitation modes are presented for flow rates  $Q = 11.5$  l/s (left column) and flow rate  $Q = 13.5$  l/s (right column) including the mode #0 representing the time-averaged cavitation field.

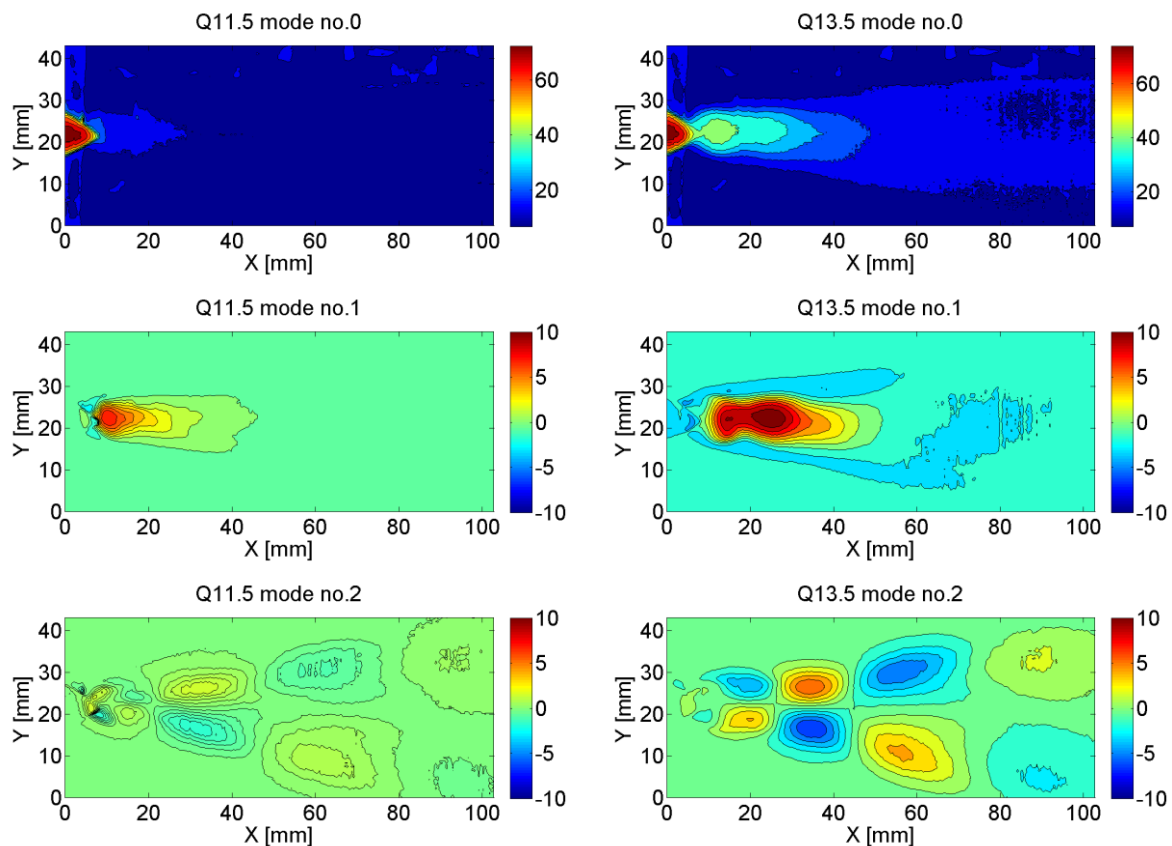


Figure 13 Cavitation modes for flow rate  $Q = 11$  (left) and 13.5 l/s (right)

## 11.1 POD OF NUMERICALLY COMPUTED PRESSURE FIELDS

In Figure 14 the POD modes are presented for the lowest and highest computed flow rates ( $Q = 5$  and  $13$  l/s) in order to present the spatio-temporal changes of the vortex structure when the flow rate increases. Besides the spatial shapes represented as the contour of  $\phi_i^k(\mathbf{x})$  the value of corresponding temporal mode frequency is added to the right corner.

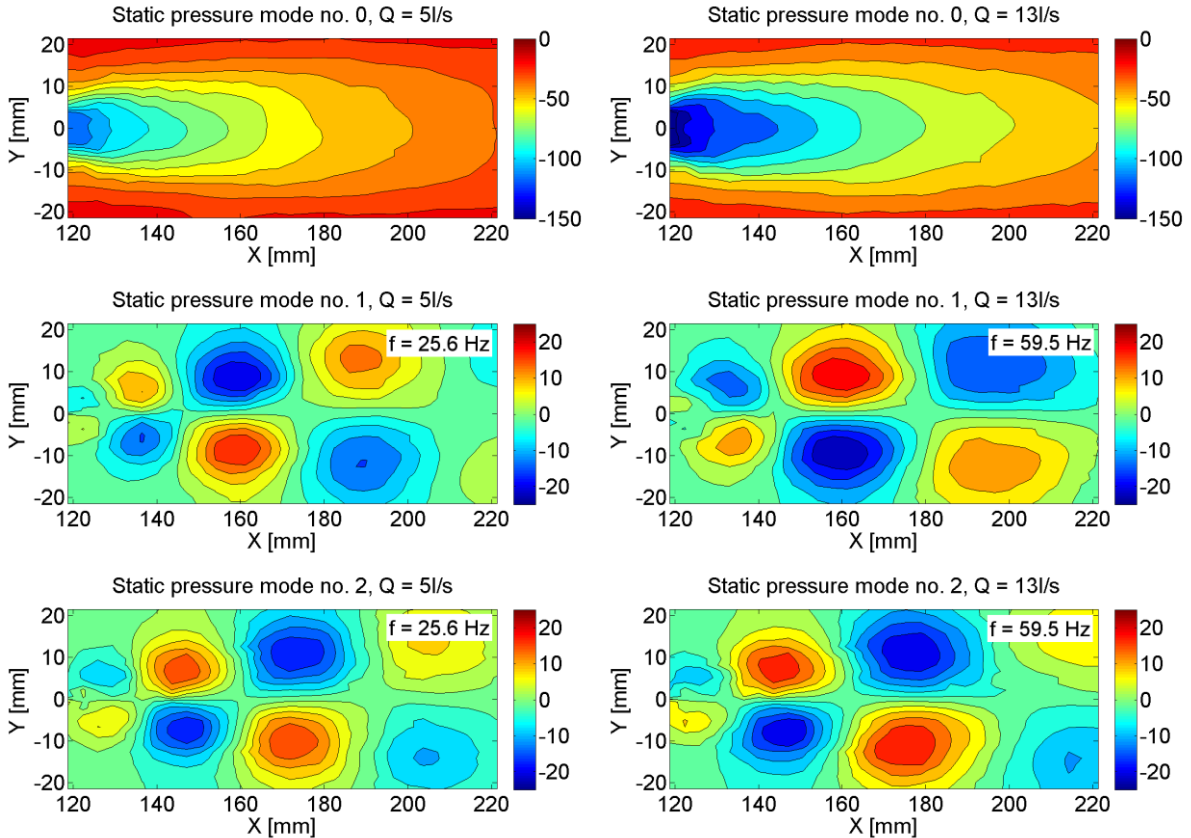


Figure 14 The first ten spatial modes of static pressure, flow rate  $Q = 5$  l/s (left) and  $Q = 13$  l/s (right)

## 12 POD ANALYSIS OF “UPT” SWIRL GENERATOR WITH THE AXIAL WATER INJECTION

On the base of author’s internship at Politehnica University of Timisoara in Romania the collaborative work arose employing the POD technique for numerical calculation of “UPT” swirl generator apparatus designed by our colleagues in Timisoara, see test case in section 4.2. This work presents utilization of POD in order to study influence of the axial water injection as a methodology used to suppress the spiral vortex dynamics.

This analysis is focused on the active control method proposed by Resiga et al. [37] employing the axial water jet injected along of the diffuser axis. In contrary with the [24] where the helical instability is suppressed by changes in the fluid

density this approach is based on the change of the mean flow. Particularly, the axial water jet method is tested on a straight draft tube using a swirl generator apparatus instead of the turbine runner [3]. Numerical computations of the jet influence on decelerated swirling flow in the diffuser for several jet discharges performed by Muntean et al. [20] are carried out in order to compare numerical results with experimental ones [5]. The data sets of velocity and pressure fields are used for the POD analysis. The computed pressure and velocity fields are further decomposed to extract the main significant modes.

## 12.1 NUMERICAL SET-UP

The three-dimensional computational domain shown in Figure 15 corresponds to the convergent-divergent section of the experimental swirl generator apparatus. The inlet boundary of the computational domain is the annular section located just downstream of the free runner while the outlet section belongs to a cylindrical extension of the divergent part. The turbulent velocity profiles used as the inflow condition in present numerical computation, together with the profiles of turbulent kinetic  $k$  energy and dissipation rate  $\varepsilon$  are results of previous numerical simulation [5]. The pressure outlet with the radial equilibrium condition is prescribed on the outlet boundary located downstream of the conical section in the extended pipe.

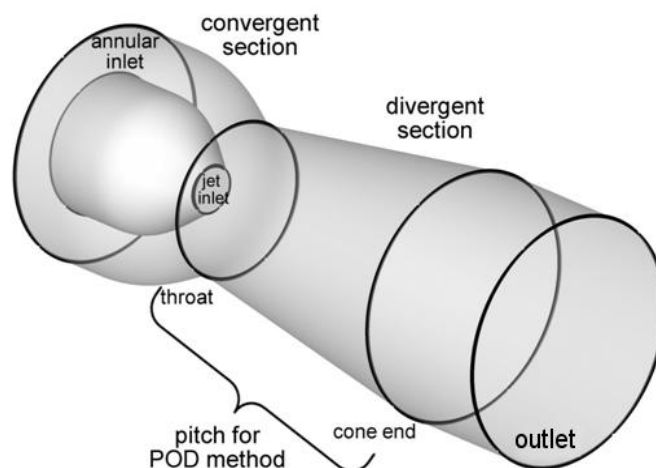


Figure 15 Three-dimensional computational domain of convergent-divergent section

The three-dimensional turbulent unsteady computation with the time step of  $\Delta t = 1.10^{-4}$  sec is carried out using the commercial software ANSYS Fluent R14 [1]. The Reynolds stress model (RSM) with second-moment closure was chosen in order to include the effect of strong turbulence anisotropy [1], [10], [31].

## 12.2 DECELERATED SWIRLING FLOWS WITH THE AXIAL WATER INJECTION

In this section the influence of the axial water jet to the pressure and radial velocity fields is discussed. The spatio-temporal behavior of the POD modes during

the axial water injection is compared with the experimental data. Firstly, the evolution of Strouhal number during the axial water injection is plotted in Figure 16 against the experimental data.

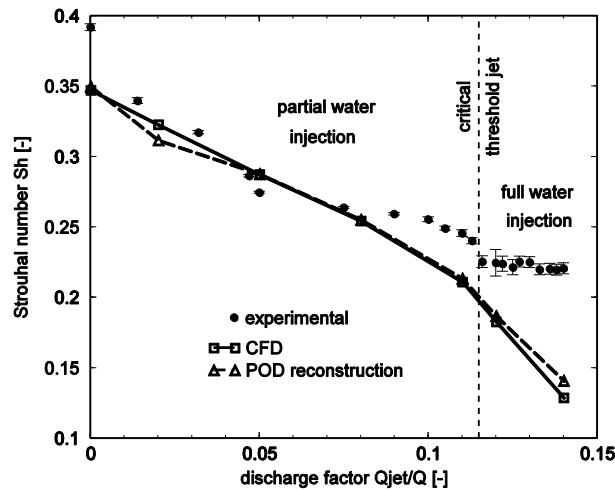


Figure 16 Strouhal number numerically computed for different values of the jet discharge against experimental data

### 12.3 5% JET DISCHARGE

At 5% jet discharge the continuous increase in eigenvalue magnitude of static pressure mode #0 and decrease in eigenvalue magnitude of modes #1 and #2 is observed, see Figure 17a. On the other hand, one can see much larger increase in eigenvalue magnitude of the radial velocity modes #1 and #2. Nevertheless the time-averaged radial velocity mode #0 increase as well. That means that the energy budget of radial velocity modes #1 and #2 increases at the expense of the rest modes which are strongly reduced, see Figure 17b. The relevant frequency spectra of both static pressure and radial velocity temporal modes are presented in Figure 18.

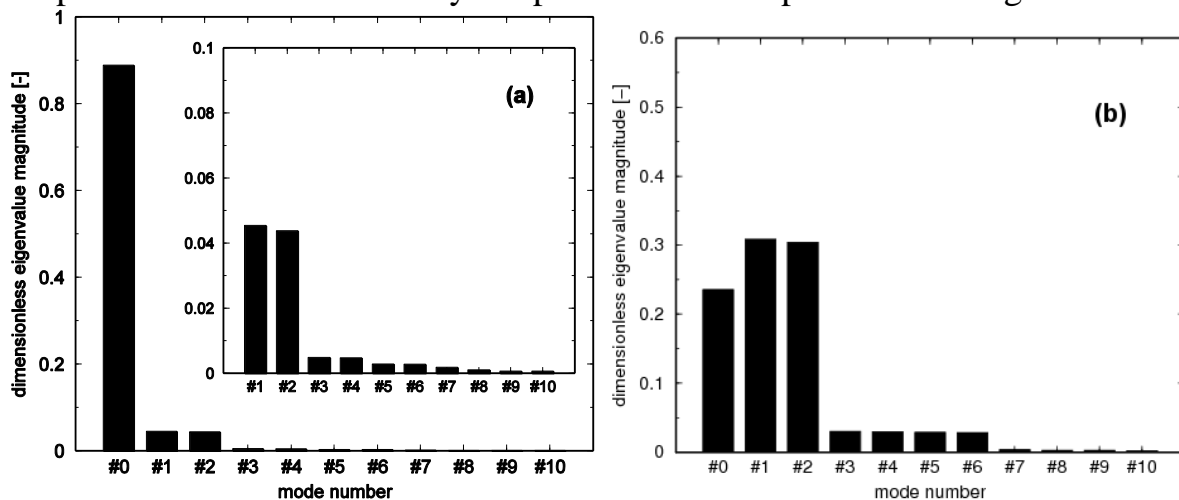


Figure 17 Dimensionless eigenvalue magnitude of the first ten static pressure modes (a) and radial velocity modes (b) at 5% jet discharge

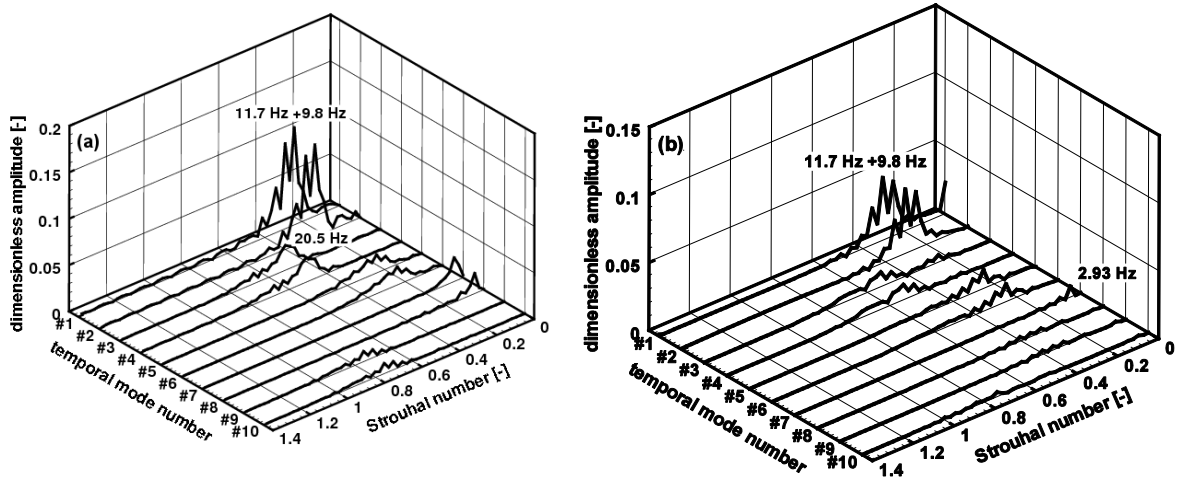


Figure 18 Power spectra of static pressure modes (a) and radial velocity modes (b) at 5% jet discharge

Positive influence of 5% jet to the flow dynamic suppression is clear from the spatial shapes of both static pressure and radial velocity mode #1. The modes are pushed further downstream to the diffuser, see Figure 19. This means that the jet discharge becomes strong enough to act on modes in the upstream part of the diffuser.

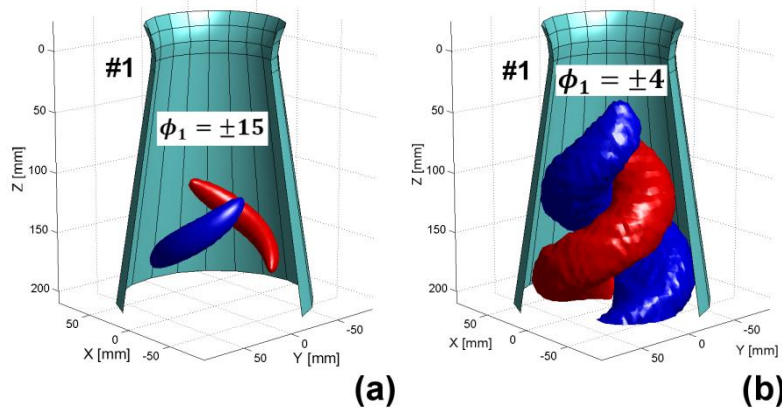


Figure 19 Spatial shape of static pressure (a) and radial velocity (b) mode #1 at 5% jet discharge

The comparison of original snapshot (iso-surface of low static pressure) with the reconstructed ones is presented in Figure 20 for case of 5% jet discharge. Consequently the reconstructed pressure fields (using 4 and 10 modes) can be correlated with the visualization (Figure 20a) on the experimental test rig. One can see that the vortex residue in the downstream part of the cone is sufficiently captured reconstructing the pressure field from 10 modes.

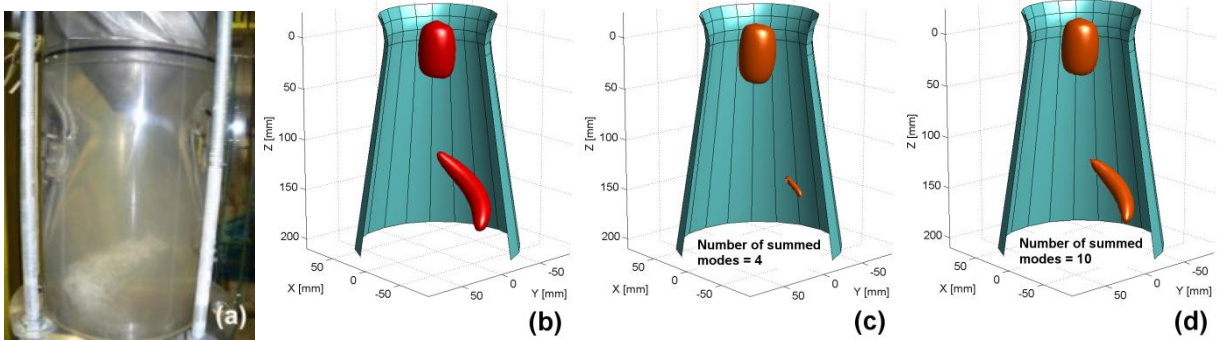


Figure 20 Vortex rope visualization on the test rig (a), the original snapshot from CFD computation (b), the reconstructed snapshots based on four modes (c) and ten modes (d), 5% jet discharge

### 13 CONCLUSIONS

This thesis aims to contribute to the study of the vortex breakdown in the field of draft tube flow. The spiral form of vortex breakdown appears when the Francis turbine is operated for lower flow rates (part load) than the optimum one. Consequently the coherent structure of vortex rope appears below the turbine runner.

The behavior of corkscrew partial load vortex strongly depends on the flow rate. While for one flow rate it can be fairly robust flow pattern rotating very uniformly for another one the very unsteady corkscrew vortex rope with transition to different shapes occurs. Nonetheless the regular movement in upstream part of the draft tube is accompanied by the dissipating process in downstream part where this coherent structure decays. In order to mimic this flow phenomenon in the easiest way the swirl generator apparatus were designed to imitate flow similar to one in the draft tube of real hydraulic turbine. The detailed description of both swirl generators is presented in section 4 . Whole thesis is divided into two main parts:

The first part of the thesis is dedicated to comprehensive experimental and computational investigation of flow generated by the swirl generator designed at Viktor Kaplan Dept. of Fluid Engineering, Brno University Technology (“BUT” swirl generator). This simplified apparatus generates swirling flow which breaks down in the diffuser to the spiral vortex with cavitating core at higher flow rates. Unlike the hydraulic turbine where the flow passes through guide vanes and runner blades (thus the mismatch between swirl generated by the guide vanes and angular momentum extracted by the turbine runner is realized) here the changes in flow pattern and behavior are realized only by the increasing or decreasing flow rate. Nonetheless the main vortex features can be established – the instability trigger leading to the spiral form of vortex breakdown, the source of synchronous and asynchronous pressure pulsations, effect of cavitating vortex core, etc. The second part of thesis is dedicated to the POD application for study of spatio-temporal features of spiral vortex. The subsections of second part are following:

- 1) The flow generated by the “BUT” swirl generator is analyzed using both experimentally and numerically obtained flow fields. These results are extension of investigation presented in the first part of thesis.
- 2) The POD is utilized in order to investigate spatio-temporal changes in the vortex dynamics when the active control (in a form of axial water jet) is applied. This study is realized on the base of collaboration using the swirl generator designed by the researchers from the Politehnica University of Timisoara in Romania (“UPT” swirl generator). The swirl generator consists of both guide vanes and free runner and the design is so that the resulting flow is similar to one encountered in the draft tube of the Francis turbine (FLINDT project) operated at partial discharge, e.g. at 70% of the best efficiency point. Both the pressure and velocity fields are investigated.

The results from well-conducted experimental measurements are usually considered as undoubtedly true (with respect to the measuring uncertainties). However, the strength of CFD is such that it provides full three-dimensional representation of the flow field. Moreover the numerically computed flow field can be expressed using various quantities (i.e. pressure, velocity components, vorticity, strain rate). It would be very difficult to record pressure in such many points in space or measure velocity vectors in such many planes to cover full three-dimensional representation of the flow experimentally. Therefore the CFD calculations, carefully verified by the experimental results, enable easy representation of this complex flow for further investigations. In this thesis the results of numerical simulations are compared with experimental ones for both swirl generator cases. Both the open-source and commercial CFD softwares were used. While the flow in “BUT” swirl generator is calculated using the OpenFOAM, the numerical data of “UPT” swirl generator are carried out in commercial ANSYS Fluent.

**The main thesis outcomes:**

- In the first part analyzing flow generated by “BUT” swirl generator was shown that the magnitude of asynchronous pulsations and its frequency decrease downstream of the diffuser well correspond for both the static pressure and velocity fields. It proves the significant link between pressure and velocity field through the Navier-Stokes equation. From the pressure measurements it was observed that the largest amplitudes and lower values of the mean static pressure are obtained for the pressure sensor p2 situated at the beginning of the cone. In this section the vortex core is the most significant which is also reflected in the steep drop of pressure recovery for higher flow rates. Very good agreement was obtained for instability of the



spiral vortex. From computed pressure field was shown that the periodically decaying character of the vortex is well captured by the numerical calculation therefore it is not consequence of any other source as a natural frequency of experimental test rig. It was shown that the synchronous part of pressure pulsations is not related only to the elbow draft tube surge but it can be also found in the straight diffusers. The complexity of decaying character of the vortex is difficult to simulate by two equation  $k$ - $\epsilon$  turbulence model, which does not affect strong turbulence anisotropy. Moreover due to disagreement in results for higher flow rates the two phase numerical simulation can be recommended for the cases where the cavitating vortex core appears. At flow rate  $Q = 13$  l/s the lowest diffuser loss coefficient, highest pressure recovery and highest diffuser efficiency is achieved in the conical section compared to other numerically investigated flow rates. Nevertheless overall energy dissipation quadratically increases with increasing flow rate. Finally the vortex rotational frequency decrease along the diffuser axis was clarified considering two reasons – increase of diffuser diameter and collapsing spiral vortex.

- The main outcomes of POD decomposition are following: The radial velocity field is very good measure of the flow instability. The spatio-temporal behavior of the static pressure modes is in excellent agreement with the one obtained from the velocity field. In some cases the POD of static pressure field can be preferable (in case of numerical data) compared to the POD of velocity field. The backward reconstruction of static pressure field executed using only the finite number of modes (e.g. consideration of only 10 most significant modes) is able to approximate the original one with sufficient accuracy. The main discrepancy in spiral vortex spatial shape is caused by neglecting of higher modes related to the small scale turbulent eddies which are responsible for the vortex rope decay in the downstream part of the cone. The quality of POD results increases with the length of sampled time.
- Advantages of POD decomposition in study of active flow control for mitigation of vortex dynamics were presented.

POD provides basis for further utilization of reduced order model (ROM), sometimes called low order dynamical model for the draft tube flow control. The ROM model is derived by projection of Navier-Stokes equation onto POD basis. One of the first applications of ROM can be found in [34] and [35].

## LITERATURE

- [1] Ansys Inc., 2011, ANSYS FLUENT 14.0 User's Guide, Canonsburg, Pennsylvania, USA.
- [2] Berkooz, G., Holmes, P., and Lumley, J.L.: 1993 "The proper orthogonal decomposition in the analysis of turbulent flows. *Annual Rev. of Fluid Mechanics* 25, pp. 539-575
- [3] Bosioc A, Susan-Resiga R. F., Muntean S, Tanasa C., (2012) Unsteady Pressure Analysis of a Swirling Flow with Vortex Rope and Axial Water Injection in a Discharge Cone. *Journal of Fluids Engineering*, vol. 134 / 081104 p. 1-11
- [4] Bosioc, A., Susan-Resiga, R. F., and Muntean, S.: Design and Manufacturing of a Convergent-Divergent Test Section for Swirling Flow Apparatus, in: *Proceedings of the 4<sup>th</sup> German – Romanian Workshop on Turbomachinery Hydrodynamics (GRoWTH)*, June 12-15, Stuttgart 2008, Germany.
- [5] Bosioc, A., Tanasa, C., Muntean, S., Susan-Resiga, R. F.: 2D LDV measurements and comparison with axisymmetric flow analysis of swirling flow in a simplified draft tube. In *Proceedings 3rd IAHR International Meeting of the Workgroup on Cavitation and Dynamic Problems in Hydraulic Machinery and Systems*, Brno, Czech Republic, October 14-16, 2009.
- [6] Brekke, H. (2010). A Review on Work on Oscillatory Problems in Francis Turbines, *New Trends in Technologies: Devices, Computer, Communication and Industrial Systems*, Meng Joo Er (Ed.), ISBN: 978-953-307-212-8
- [7] Dörfler, P., Sick, M. and Coutu, A. *Flow-Induced Pulsations and Vibration in Hydraulic Machinery*, DOI: 10.1007/978-1-4471-4252-2\_1, Springer-Verlag London 2013.
- [8] Frunzaverde, D., Muntean, S., Marginean, G., Campian, V., Marsavina, L., Terzi, R., and Serban, V., 2010, "Failure Analysis of a Francis Turbine Runner", *IOP Conf. Series: Earth and Environ. Sci.*, **12**, 012115, pp. 1-10, doi: 10.1088/1755-1315/12/1/012115.
- [9] Grinberg, L., Yakhot, A., Karniadakis, G. E.: Analyzing Transient Turbulence in a Stenosed Carotid Artery by Proper Orthogonal Decomposition, *Annals of Biomedical Engineering*, Vol. 37, No. 11, (2009) pp. 2200–2217
- [10] Jawarneh, A. M., Vatistas, G. H. (2006) Reynolds Stress Model in the Prediction of Confined Turbulent Swirling Flows, in: *ASME Journal of Fluid Engineering*, Vol. 128, p.p.1377-1382.

- [11] Kellnerová, R., Kukačka, L., Juračková, K., Uruba, V., Jaňour, Z.: PIV measurement of turbulent flow within a street canyon: Detection of coherent motion. *J. Wind Eng. Ind. Aerodyn.* 104–106 (2012) pp.302–313
- [12] Kirschner, O., Schmidt, H., Ruprecht, A., Mader, R., and Meusburger, P., 2010, “Experimental Investigation of Vortex Control with an Axial Jet in the Draft Tube of a Model Pump-Turbine”, IOP Conf. Series: Earth and Environ. Sci., **12**, 012092, pp. 1-9, doi: 10.1088/1755-1315/12/1/012092.
- [13] Kjeldsen, M., Olsen, K., Nielsen, T., and Dahlhaug, O., 2006, “Water Injection for the Mitigation of draft Tube Pressure Pulsations”, Proc. 1st IAHR International Meeting of Working Group on Cavitation and Dynamic Problems in Hydraulic Machinery and Systems, Barcelona, Spain. pp. 1-11.
- [14] Kurokawa, J., Kajigaya, A., Matusi, J., and Imamura, H., 2000, “Suppression of Swirl in a Conical Diffuser by Use of J-Groove”, Proc. 20th IAHR Symposium on Hydraulic Machinery and Systems, Charlotte, NC, USA, Paper No. DY-01, pp. 1-10.
- [15] Kurokawa, J., Imamura, H., and Choi Y.-D., 2010, “Effect of J-Groove on the Suppression of Swirl Flow in a Conical Diffuser”, *Journal of Fluids Engineering – Transaction of ASME*, **132**(7), 071101, pp. 1-8, doi: 10.1115/1.4001899
- [16] Lucca-Negro, O., O’Doherty, T. (2001) Vortex breakdown: a review, in: *Annual Review of Fluid Mechanics*, 10, 221-246, 1978.
- [17] Lumley JL 1967 The structure of inhomogeneous turbulence. In: *Yaglom AI Tatarski VI (eds) Atmospheric turbulence and wave propagation* (Moscow: Nauka)
- [18] Mayer, K. E., Pedersen, J. M., Özcan, O.: A turbulent jet in crossflow analysed with proper orthogonal decomposition. *J. Fluid Mech.* (2007), vol. 583, pp. 199–227. (2007)
- [19] Miyagawa, K., Sano, T., Kunimatsu, N., Aki, T., and Nishi, M., 2006, “Flow Instability With Auxiliary Parts in High Head Pump – Turbines”, Proc. 23rd IAHR Symposium on Hydraulic Machinery and Systems, Yokohama, Japan, Paper F307.
- [20] Muntean, S., Susan-Resiga, R., and Bosioc, A., 2009, “Numerical investigation of the jet control method for swirling flow with precessing vortex rope”, Proc. 3rd IAHR International Meeting of the Workgroup on Cavitation and Dynamic Problems in Hydraulic Machinery and Systems, Brno, Czech Republic. Paper B2, pp. 1-10.
- [21] Nishi, M., Wang, X. M., Yoshida, K., Takahashi, T., and Tsukamoto, T., 1996, “An Experimental Study on Fins, Their Role in Control of the Draft Tube Surging,” *Hydraulic Machinery and Cavitation*, E. Cabrera, V. Espert, and F.

Martinez (eds.), Kluwer Academic Publishers, Dordrecht, The Netherlands, pp. 905–914.

[22] Oberleithner, K., Sieber, M., Nayeri, C. N., Paschereit, C. O., Petz, C., Hege, H.-C., Noack, B. R., Wagnanski I.: Three-dimensional coherent structures in a swirling jet undergoing vortex breakdown: stability analysis and empirical mode construction. *J. Fluid Mech.*, 32 pages. (2011)

[23] Oberleithner, K., Sieber, M., Nayeri, C. N., Paschereit, C. O.: On the control of global modes in swirling jet experiments. *Journal of Physics: Conference Series* 318 (2011)

[24] Oberleithner, K., Terhaar, S., Rukes, L., Paschereit, C. O. Why Non Uniform Density Suppresses the Precessing Vortex Core, *J. Eng. Gas Turbines Power*. Vol. 135, No. 12, 2013

[25] Oudheusden, B. W., Scarano, F., Hinsberg, N. P., Watt, D. W.: Phase-resolved characterization of vortex shedding in the near wake of a square-section cylinder at incidence, *Experiments in Fluids* (2005) 39: 86–98 DOI 10.1007/s00348-005-0985-5

[26] Pappilon, B., Sabourin, M., Couston, M., and Deschenes, C., 2002, “Methods for Air Admission in Hydro Turbines,” *Proc. 21st IAHR Symposium on Hydraulic Machinery and Systems*, Lausanne, Switzerland, pp. 1–6.

[27] Perrin, R., Braza, M., Cid, E., Cazin, S., Barthet, A., Servain, A., Mockett, C., Thiele, F.: Obtaining phase averaged turbulence properties in the near wake of circular cylinder at high Reynolds number using POD. *Exp Fluids* (2007) 43, pp.341–355.

[28] Qian Z.D., Li W., Huai W.X., and Wu Y.L., 2012, “The effect of the runner cone design on pressure oscillation characteristics in a Francis hydraulic turbine”, *Proc. IMechE, Part A: J. Power and Energy*, **226**(1), pp. 137-150, doi: 10.1177/0957650911422865

[29] Rudolf P 2010 Eigenmode shapes of the swirling flow in a diffuser. *Proceedings of EUROMECH Fluid Mechanics Conference*, Bad Reichenhall

[30] Rudolf P and Jizdný M 2011 Decomposition of the swirling flow fields. *Proceedings of the 4th International Meeting on Cavitation and Dynamic Problems in Hydraulic Machinery and Systems*, Belgrade

[31] Rudolf P., Skoták A. – Unsteady flow in the draft tube with elbow. Part B – Numerical investigation, *WG on the behavior of hydraulic machinery under steady oscillatory conditions*, Trondheim 2001

[32] Rudolf, P. (2009) Connection between inlet velocity field and diffuser flow instability, in: *Applied and Computational Mechanics*, Vol. 3, No. 1, pp. 177 – 184.

[33] Rudolf, P., Štefan, D.: 2012 Decomposition of the swirling flow field downstream of Francis turbine runner. *IOP Conf. Ser.: Earth Environ. Sci.* 15

[34] Rudolf, P., Štefan, D. Reduced order model of draft tube flow. *IOP Conference Series: Earth and Environmental Science*, 2014, Vol. 22, No. 1

[35] Rudolf, P., Štefan, D., Klas, R. 2015 Spatio-Temporal Description of the Swirling Flow in Hydraulic Turbine Draft Tube. *Wasserwirtschaft*, 2015,(13), pp. 18-22.

[36] Sirovich, L.: 1987 Turbulence and the dynamics of coherent structures. Part I: Coherent structures. *Quarterly of Applied Mathematics XLV*, pp. 561-571

[37] Susan-Resiga, R., Vu, T.C., Muntean, S., Ciocan, G.D., and Nennemann, B., 2006, “Jet Control of the Draft Tube in Francis Turbines at Partial Discharge”, Proc. 23rd IAHR Symposium on Hydraulic Machinery and Systems, Yokohama, Japan, Paper F192, pp. 1-14.

[38] Susan-Resiga, R., and Muntean, S., 2008, “Decelerated Swirling Flow Control in the Discharge Cone of Francis Turbines”, Proc. 4th International Symposium on Fluid Machinery and Fluid Mechanics, Beijing, China, Paper IL-18, pp. 89-96, doi: 10.1007/978-3-540-89749-1\_12

[39] Susan-Resiga, R.F., Muntean, S., Hasmatuchi, H., Anton, I., Avellan, F., Analysis and Prevention of Vortex Breakdown in the Simplified Discharge Cone of a Francis Turbine. *Journal of Fluids Engineering*, Vol. 132. (2010)

[40] Susan-Resiga, R. F., Muntean, S., Tanasa, C., Bosioc, A. (2008) Hydrodynamic Design and Analysis of a Swirling Flow Generator, in: *Proceedings of the 4<sup>th</sup> German – Romanian Workshop on Turbomachinery Hydrodynamics (GRoWTH)*, June 12-15, 2008, Stuttgart, Germany.

[41] Susan-Resiga R, Muntean S, Vu T C, Ciocan G D and Nennemann B 2006 Jet Control of the Draft Tube Vortex Rope in Francis Turbines at Partial Discharge *Proc. of the 23rd IAHR Symp. on Hydr. Machin. and Syst.* (Yokohama, Japan) p 192

[42] Thicke, R.H., 1981, “Practical Solutions for Draft Tube Instability”, *International Water Power and Dam Construction*, **33**(2), pp. 31-37.

[43] Vevke, T., 2004, “An Experimental Investigation of Draft Tube Flow,” Ph.D thesis, Norwegian University of Science and Technology, Trondheim, Norway.

[44] Wu Y.L., Li S.C., Liu S.H., Dou, H.-S., and Qian Z.D., 2013, *Vibration of Hydraulic Machinery*, Springer Verlag.

# CURRICULUM VITAE

**Name:** David ŠTEFAN

**Date and place of birth:** 5. 2. 1987, Brno, Czech Republic

Education:

2011 – 2015      *Doctoral degree* - Brno University of Technology, Faculty of mechanical engineering, specialization Design and Process Engineering

2009 – 2011      *Engineering degree* - Brno University of Technology, Faculty of mechanical engineering, specialization Fluid Engineering

2006 – 2009      *Bachelor degree* - Brno University of Technology, Faculty of mechanical engineering, specialization Mechanical engineering

2002 – 2006      Secondary School and Vocational Technical School in Brno, Sokolská 1, specialisation: Industries – 2D and 3D drawings

## **Research visits and internships:**

August – September 2012      IHS, University Stuttgart, Germany, within HPC-Europa2 programme

October – December 2012      Department of Hydraulic Machinery, Politehnica University of Timisoara, Romania, within ERASMUS programme

## **ABSTRACT**

This work deals with study of swirling flows where the spiral vortical structure appears. The main relation is to flow seen in the draft tube cone of hydraulic turbines operated out of the design point (i.e. best efficiency point). In this cases large coherent vortex structure (vortex rope) appears and consequently high pressure pulsations are propagated to the whole machine system leading to possible restriction of turbine operation. This flow features are consequence of flow instability called vortex breakdown in case of Francis turbine operated at part load (flow rate lower than optimal one).

The present study is carried out using simplified device of swirl generator in order to access similar flow conditions as can be found in real hydraulic turbines. Both the dynamic and dissipation effect of spiral vortex breakdown are investigated.

The first part of thesis deals with spiral form of vortex breakdown. The experimentally measured velocity profiles (LDA) and wall static pressures are correlated with numerical simulations carried out using open-source CFD package OpenFOAM 2.2.2. The high speed camera recording of cavitating vortex core is used to obtain image ensemble for further post-processing. The dissipation effect of spiral vortex structure is in detail discussed based on computed flow fields.

The second part of thesis is dedicated to the application of POD decomposition to the study of spatio-temporal features of spiral vortex dynamics. Firstly the POD is applied to the both the experimentally obtained image ensemble of cavitating vortex and numerically computed static pressure fields. Secondly the comprehensive analysis of spiral vortex mitigation effect by the axial water jet is analyzed. The collaborative study employing the swirl generator apparatus designed by the researchers from Politehnica University of Timisoara in Romania is performed and changes in spatio-temporal vortex dynamic are studied. In this study the numerical data (in a form of three-dimensional pressure and velocity fields) are obtained using commercial CFD software ANSYS Fluent R14.